Molecular Immunology 112 (2019) 59–71

Contents lists available at ScienceDirect

Molecular Immunology

journal homepage: www.elsevier.com/locate/molimm

Molecular structure, expression, and bioactivity of B-cell–activating factor of the TNF family (BAFF) and its receptor BAFF-R in cats (*Felis catus*)

Ming Sang[a,b,c,1], Jianfeng Li[c,d,1], Zhiheng Wei[a,c,1], Xiaolong Wu[a,c,1], Zhiguo Wang[d], Lei Ma[c], Hongzhen Liu[c], Shuangquan Zhang[c,*], Jiaxin Zhang[a,c,*]

[a] School of Food Science and Pharmaceutical Engineering, Nanjing Normal University, Nanjing 210046, China
[b] Laboratory of Cellular and Molecular Biology Jiangsu Province Institute of Traditional Chinese Medicine Nanjing, China
[c] Jiangsu Province Key Laboratory for Molecular and Medical Biotechnology, Life Sciences College, Nanjing Normal University, Nanjing 210046, China
[d] Institute of Aging Research, School of Medicine, Hangzhou Normal University, Hangzhou, Zhejiang Province 311121, China

ARTICLE INFO

Keywords:
BAFF
BAFF-R
Cat
Molecular structure
Immunology function
Ligand–receptor interactions

ABSTRACT

B-cell survival depends on signals induced by binding of B-cell activating factor (BAFF) to its receptor (BAFF-R). In this study, the full-length cDNAs of cat BAFF (cBAFF) and BAFF-R (cBAFF-R) were amplified from the spleen by reverse transcription PCR. The open reading frame of cBAFF cDNA encodes a protein of 285 amino acids containing a predicted transmembrane domain and a furin protease cleavage site, similar to mammalian, avian, and reptile BAFFs. The cBAFF-R gene encodes a 189 amino acid protein. Real-time quantitative PCR analyses revealed that the two genes are predominantly expressed in the spleen. csBAFF, EGFP/csBAFF, and cBAFF-R were efficiently expressed in *Escherichia coli* BL21 (DE3), as confirmed by sodium dodecyl sulfate-polyacrylamide gel electrophoresis and Western blotting analyses. After purification, the EGFP/csBAFF fusion protein showed a fluorescence spectrum similar to that of EGFP. Confocal laser scanning microscopy showed that EGFP/csBAFF bound to its receptor. *In vitro*, csBAFF promoted the survival of cat and mouse splenic B cells with/without a priming agent (*Staphylococcus aureus* Cowan 1, SAC) or anti-mouse IgM. Furthermore, it stimulated the survival of mouse B cells, similar to msBAFF. Recombinant cBAFF-R blocked the function of sBAFF *in vitro*. These findings indicate that csBAFF plays an important role in the survival of cat B cells and has functional cross reactivity between cats and other mammals, and suggest a role for the BAFF–BAFF-R system in regulating B-cell survival. Therefore, BAFF and BAFF-R show promise for enhancing the immune systems of animals.

1. Introduction

The B-cell–activating factor of the TNF family (BAFF, also known as BLyS, TALL-1, THANK, zTNF4, and TNFSF13b) is a 285 amino acid transmembrane protein that exists as both a membrane and a cleaved 152 amino acid soluble form (JA et al., 2000; Moore et al., 1999; Mukhopadhyay et al., 1999; Schneider et al., 1999; Shu et al., 1999; Tribouley et al., 1999) and plays a major role in Bcell survival, proliferation, and differentiation (Rolink et al., 2015). BAFF is a type II transmembrane protein that forms biologically active trimers (Bodmer et al., 2002; JS et al., 2001). BAFF is synthesized as a membrane-bound protein that can be processed into a soluble form after cleavage at a furin consensus sequence, a site that can be recognized by several proteases of the pro-protein convertase family (Kowalczyk-Quintas et al., 2018; Schneider et al., 1999). BAFF interacts with three cell-surface receptors from the TNF receptor superfamily (TNFRSF): BAFF-receptor (BAFF-R, also known as BR3, CD268, and TNFRSF13C), B-cell maturation antigen (BCMA and TNFRSF17), and transmembrane activator and calcium modulator and cyclophilin ligand (TACI, CD267, and TNFRSF13B) (Gross et al., 2000; Marsters et al., 2000; Shu and Johnson, 2000; Thompson et al., 2001, 2000), all of which are expressed primarily in B cells. Except for bone marrow plasma cells, BAFF-R is expressed in other B cells (Darce et al., 2007; Guan et al., 2004), BAFF-R is also continuously expressed in regulatory T cells

Abbreviations: cDNA, DNA complementary to RNA; IPTG, isopropyl-b-D-thiogalactoside; RT-PCR, reverse transcription-polymerase chain reaction; GAPDH, glyceraldehyde phosphate dehydrogenase; csBAFF, cat soluble BAFF; EGFP, enhanced green fluorescent protein; SDS-PAGE, sodium dodecyl sulfate polyacrylamide gel electrophoresis; TNF, tumor necrosis factor; IgG, immunoglobulin G; IgM, immunoglobulin M; SAC, *Staphylococcus aureus* Cowan 1; PI, propidium iodide

* Corresponding authors.
E-mail addresses: zhangshuangquan@njnu.edu.cn (S. Zhang), 45239@njnu.edu.cn (J. Zhang).
[1] These authors contributed equally to this work.

https://doi.org/10.1016/j.molimm.2019.04.031
Received 2 March 2019; Accepted 30 April 2019
Available online 08 May 2019

(Mackay and Leung, 2006) and naive and memory subsets of $CD4^+$ and $CD8^+$ cells (Guan et al., 2004). BCMA is most likely relevant for the later stages of B cell maturation or survival, *i.e.*, for $CD38^+$ plasmablasts (Avery et al., 2003) and germinal center B cells. Furthermore, BCMA is expressed by tonsillar memory B cells in addition to plasma cells from both tonsil and bone marrow tissues (Darce et al., 2007). In addition, the expression of BCMA is absent in naive B cells and peripheral blood and memory B cells (Darce et al., 2007). TACI is predominantly expressed by memory B cells and tonsillar and bone marrow plasma cells, although to a lesser degree in the latter population (Darce et al., 2007). A small subset of $CD27^{neg}$ naive B cells also express low levels of TACI and this has been observed in both blood and tonsil tissues (Darce et al., 2007). Likewise, TACI is expressed only weakly in a small subset of peripheral B cells. However, it may play an important role in some aspects of B cell maturation or function within the spleen, because transitional type 2 and marginal zone B cells express high levels of TACI (Guan et al., 2004). BAFF is the sole ligand for BAFF-R, while it shares receptor specificity for TACI and BCMA with a proliferation-inducing ligand (APRIL) (Mackay and Ambrose, 2003). BAFF-R, TACI, and BCMA display unique but overlapping expression patterns, functional analyses have revealed distinct roles for these three receptors in mediating BAFF (and APRIL) signals, and BAFF-R specifically binds to BAFF, which is the major receptor involved in triggering BAFF-induced B-cell survival (Bossen and Schneider, 2006; Mackay et al., 2007). Stimulation of BAFF-R potently activates the alternative NF-κB2 pathway, which provides one of the bases for the effects of BAFF on B-cell survival (Vallabhapurapu et al., 2008). The crystal structure of the functional soluble part of human BAFF (hsBAFF) has an unusually long D-E loop (also termed the "flap") compared to other TNF-family members, which forms a region that might be important for receptor binding and virus-like assembly (Karpusas et al., 2002; Liu et al., 2002). BAFF plays a central role in B-cell maturation, survival, and Tcell activation, as well as in autoimmune diseases (Bossen and Schneider, 2006; Mackay et al., 2007). BAFF-transgenic mice have increased numbers of mature B cells in circulation, hyperglobulinemia, and lupus-like nephritis, secondary to enhanced survival of autoreactive B cells, consistent with *in vitro* observations (Khare et al., 2000; Mackay et al., 1999; Ng et al., 2005). Agents that block BAFF have proven to be highly effective for the treatment of certain autoimmune conditions in mice (Sutherland et al., 2006; Tangye et al., 2006). By contrast, BAFF-deficient mice exhibit dramatically reduced B-cell numbers peripherally and impaired development of germinal-center responses (Rahman et al., 2003; Schiemann et al., 2001). BAFF-R-deficient mice have significantly reduced numbers of mature peripheral B cells (Lilian et al., 2006). As for the expression of most B-cell subsets (Mackay and Schneider, 2009), BAFF-R is expressed by many low-grade B-cell neoplasms and some diffuse large B-cell lymphomas (Nakamura et al., 2005). Interestingly, surface BAFF-R is downregulated in chronic lymphocytic leukemia (Mihalcik et al., 2010) and upregulated in precursor B-lineage acute lymphoblastic leukemia (Parameswaran et al., 2010). Although the mechanism remains unclear, an understanding of BAFF-R dysregulation may offer novel diagnostic and therapeutic opportunities for these cancers.

Cats are common family pets globally. Thus, it is important to enhance their immune systems, particularly of rare breeds. In this study, to gain further insight into the evolution of BAFF, we cloned the full-length cDNAs of cBAFF and cBAFF-R, investigated their expression profile, and produced bioactive recombinant csBAFF and cBAFF-R to determine their bioactivity. This is the first *in vitro* characterization of cBAFF and BAFF-R, and the findings show that csBAFF could be used to enhance the immune systems of cats.

2. Materials and methods

2.1. Animals and cell preparation

Healthy male Chinese *Felis catus* about 8 months old and weighing 2–3 kg were purchased from Red-Sun Breed Co. Ltd., Jiangsu, China. Lymphocytes from their spleens were separated by density centrifugation on Ficoll-Paque (Pharmacia Biotech, Piscataway, NJ). B cells were isolated from the spleens of mice using the B-cell–specific antibody CD19 coupled to magnetic beads (Miltenyi Biotec, Bergisch Gladbach, Germany), as described previously (Tedder, 2009). Both types of spleen cell (cat and mouse) were maintained in Roswell Park Memorial Institute (RPMI)-1640 medium with penicillin/streptomycin (Gibco-BRL; Gibco/Life Technologies, Carlsbad, CA) supplemented with 10% fetal bovine serum (FBS) at 37 °C in a CO_2 incubator.

Use of animals in this study was approved by the Scientific Ethics Committee of Nanjing Normal University.

2.2. RNA isolation and reverse transcription polymerase chain reaction

Total RNA was extracted using TRIzol reagent (Invitrogen/Life Technologies) according to the standard protocol and DNase-treated using RNase-free DNase set (QIAGEN, Germany) following the manufacturer's instructions. First-strand cDNA was synthesized from 1 μg RNA isolated from cat spleens using AMV Reverse Transcriptase XL (Clontech/Takara Bio, Mountain View, CA) according to the manufacturer's protocol. A pair of degenerate primers, cBAFF-1 and cBAFF-2 (Table 1), whose design was based on regions of high homology among the sequences of human, mouse, and bovine BAFF analyzed using ClustalW software, was used for reverse transcription polymerase chain reaction (RT-PCR). The RT-PCR conditions (30 cycles) were as follows: denaturing for 30 s at 94 °C, annealing for 30 s at 55 °C, and extension for 1 min at 72 °C. Within each experiment, samples with no template, no primers, and no RT controls were used to detect possible contamination.

2.3. Rapid amplification of cDNA ends (RACE)

RACE was used to generate the full-length cDNA of the cBAFF mRNA sequence, including the 3′ and 5′ untranslated regions (UTRs). Briefly, two specific primers, cBAFF-3′GSP1 and cBAFF-3′GSP2 (Table 1), were synthesized based on the cDNA sequence obtained by the internal amplification described above. For each 5′ and 3′ RACE, the cDNA was synthesized according to the manufacturer's protocol (Smart RACE cDNA Amplification Kit; Clontech/TaKaRa Bio).

2.4. Molecular cloning of full-length cBAFF and cBAFF-R cDNA

The full-length cBAFF cDNA was generated by long-distance PCR using the Advantage 2 Polymerase Mix (Clontech/Takara Bio) with the primers CB-1 and CB-2 (Table 1) designed using the distal ends of the 5′ and 3′ RACE products, respectively. The procedures were as follows: 94 °C for 5 min followed by 35 cycles (94 °C for 30 s, 58 °C for 30 s, and 68 °C for 1.5 min). The full-length cDNA sequence of cBAFF was deduced from eight independent clones. The full-length cBAFF-R cDNA was generated by long-distance PCR using the Advantage 2 Polymerase Mix (Clontech/TaKaRa Bio) with the primers cBAFF-R-1 and cBAFF-R-2 (Table 1). The procedures were as follows: 94 °C for 5 min followed by 35 cycles (94 °C for 30 s, 58 °C for 30 s, and 68 °C for 1 min). Within each experiment, samples with no template, no primers, and no RT controls were used to detect contamination. The full-length cDNA sequence of cBAFF-R was deduced from those of eight independent clones.

Table 1
Sequences of the primers used in this study.

Primer	Direction	Nucleotide sequence (5'-3')
cBAFF-1	Forward	GTCNCCTGTNCAGNGTGGNCNTCCTGC (N = A,T, G, C)
cBAFF-2	Reverse	GGANCAANTTCNCCAGNCTCANTTCGT(N = A,T, G, C)
cBAFF-3'GSP-1	Forward	TAAAGCGGGTCCTGCTATTCAAGTTC
cBAFF-3'outer	Reverse	GGTGAAAGAAACCGGTTACTTCTTTAT
cBAFF-3'GSP-2	Forward	TCTGGGTACCGCAAAAGCATTAGG
cBAFF-3'outer	Reverse	CGTCTTTGGGGACGAACTGAGTCTGGT
UPM	Forward	CTAATACGACTCACTATAGGGCAAGCAGTGGTATCAACGCAGAGT(long) CTAATACGACTCACTATAGGGC(short)
cBAFF-5'GSP-1	Reverse	AGGGCCCGGCTCAGCCCGAAGCTCGCG
NUP	Forward	AAGCAGTGGTATCAACGCAGAGT
cBAFF-5'GSP-2	Reverse	GCTCCCCAGCTCGGCTTGCAGGACGG
CB-1	Forward	ATGGAGGGCTGCGCGGAAGGCGAGCG
CB-2	Reverse	TCACAGAAGTTTCAATGCTCCAAAA
cBAFF-R-1	Forward	ATGGGCAGCCGGAGGAGAGGTGCCA
cBAFF-R-2	Reverse	CTACTGTTGCTCAGGGCCAGCAGTC
P1	Forward	CGCCGCTCTGGATCCCGAAGACACAGTCA
P2	Reverse	CCC*AAGCTT*CAGAAGTTTCAATGCTCCAAAAAA
P3	Forward	TCAGGA*CATATG*ATGGGCAGCCGGAGGAG
P4	Reverse	ACTGAG*GGATCC*CTGTTGCTCAGGGCCAGCAG
A1	Forward	TCAGGA*CATATG*GTGAGCAAG
A2	Reverse	*GCTGCCACCTCCACC*GCTACCGCCGCCTCCCTTGTACAGCTC
A3	Forward	*GGTGGAGGTGGCAGC*GCCGCTCTGGATCCCGA
A4	Reverse	CCC*AAGCTT*CAGAAGTTTCAATGCTCCAAA
Q1	Forward	CGGGCAGGTTTTATACACGG
Q2	Reverse	GATGCCAGCGGAATAACAGG
Q3	Forward	GGACCGGGTAAGAGTCGAC
Q4	Reverse	GTTGCATCATAGCCTCCCAC
Q5	Forward	CATTGCCCTCAACGACCACTTTGTC
Q6	Reverse	CTCCTTGGAGGCCATGTGGACCATG

2.5. Bioinformatics analyses

Searches for nucleotide and protein sequence similarities were conducted using the BLAST algorithm at the National Center for Biotechnology Information (http://www.ncbi.nlm.nih.gov/blast). The putative promoter sequence was analyzed *in silico* with PROSCAN ver. 1.7 software from Web Promoter Scan Service (http://www-bimas.cit.nih.gov/molbio/proscan/). The deduced amino acid sequence was analyzed using the Expert Protein Analysis System (http://www.expasy.org/), and the protein domain features of cBAFF and cBAFF-R were determined using the Simple Modular Architecture Research Tool (http://smart.embl-heidelberg.de/). Isoelectric point and molecular weight predictions were performed using the following website: http://web.expasy.org/protparam/. Real-time quantitative PCR (qPCR) primer pairs were designed manually based on the guidelines included with Primer Express 2.0 software (Applied Biosystems/Life Technologies).

2.6. Phylogenetic analyses of cBAFF and cBAFF-R

Phylogenetic trees for cBAFF and cBAFF-R were constructed based on the proportion of amino acid differences (p-distance) and complete gap deletion using the neighbor-joining method with MEGA 5.0. The reliability of the tree was assessed by bootstrapping with 1000 bootstrap replications. The phylogeny signals of the nucleotide and amino acid sequences were evaluated using TREE-PUZZLE ver. 5.2 (Schmidt et al., 2002).

2.7. qPCR analyses of gene expression

To evaluate the tissue expression profile of cBAFF and BAFF-R, first-strand cDNAs were synthesized from RNA isolated from different cat tissues using the Prime Script Real Time Quantitative PCR Kit (Clontech/TaKaRa Bio) according to the standard protocol. A variable amount of cDNA was used in a total volume of 50 µL PCR mixture containing SYBR Premix Ex Taq (Clontech/Takara Bio). A pair of primers (Q1 and Q2, Table 1) was used to amplify a 163 bp fragment of cBAFF, and another pair of primers (Q3 and Q4, Table 1) was used to amplify a 203 bp fragment of cBAFF-R. PCR conditions were as follows: 95 °C for 30 s; 40 cycles (95 °C for 5 s, 60 °C for 30 s); and 95 °C for 15 s, 60 °C for 30 s, and 95 °C for 15 s. Endogenously expressed cat GAPDH mRNA (GenBank Accession No. NP_001009307.1) was used as the internal control. The Q5 and Q6 primers (Table 1), with the above-described PCR conditions, were used to amplify a 167 bp fragment of cat GAPDH. Within each experiment, samples with no template, no primers, and no RT controls were used to detect contamination.

2.8. Construction, expression, and purification of csBAFF, EGFP/csBAFF, and cBAFF-R

The DNA fragment encoding the extracellular region of cBAFF (aa 132–285), also known as the soluble form of cBAFF (csBAFF), was amplified by PCR using the primers P1 and P2 (Table 1). The resulting PCR product was digested with *Stu*I and *Hind*III and ligated into the pSUMO plasmid at the corresponding restriction sites. The resulting recombinant plasmid was named pSUMO–csBAFF.

Luria–Bertani (LB) medium (100 mL; 50 µg/mL kanamycin) was inoculated (1:50) with a non-induced confluent bacterial suspension and grown at 37 °C with vigorous shaking until reaching an optical density at 600 nm (OD600) of 0.4. Then expression was induced by adding 0.2 mM isopropyl-D-1-thiogalactopyranoside (IPTG) and the cultures were incubated for 48 h at 15 °C with shaking at 150 rpm [27]. The soluble protein in the supernatant was collected by refrigerated centrifugation after hypersound quassation. Finally, the target protein was purified using His-Bind columns (Qiagen, Venlo, The Netherlands) according to the manufacturer's instructions.

Based on the EGFP and csBAFF sequences and using the pET-28a vector and overlap method, we designed four primers (Table 1) for PCR. The EGFP gene was cloned by PCR using the primers A1 and A2 with an extra *Nde*I recognition site at its 5′ end. PCR was performed for 30 cycles at 94 °C for 30 s, 55 °C for 30 s, and 72 °C for 60 s. The primers A3 and A4 were used to amplify the DNA sequence of csBAFF, which

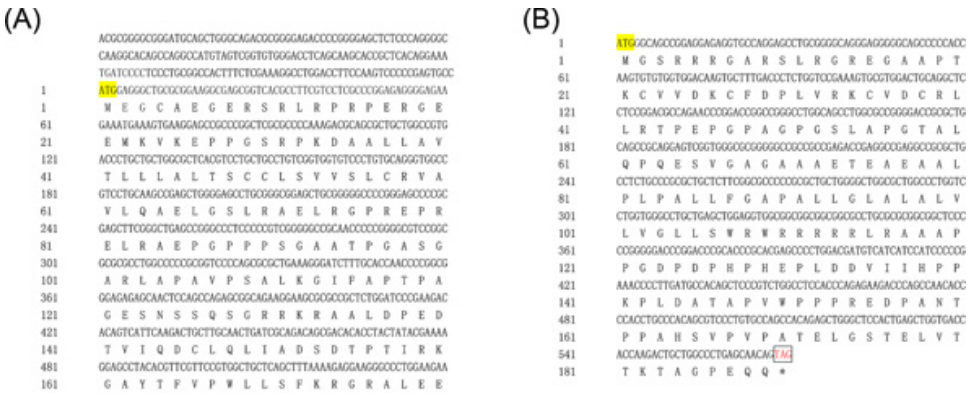

Fig. 1. (A) Nucleotide and deduced amino acid sequences of cat BAFF cDNA (GenBank Accession No. MH151314). The stop codon TGA is boxed and marked (*). The entire deduced amino acid sequence is depicted in single-letter code beneath the corresponding nucleotide sequence. Furin cleavage sites are indicted by gray shading. **(B)** Nucleotide and deduced amino acid sequences of cat BAFF-R cDNA (GenBank Accession No. MH244349). The stop codon TGA is boxed and marked (*). The entire deduced amino acid sequence is depicted in single-letter code beneath the corresponding nucleotide sequence.

contains a *Hind*III recognition site at its 3′ end. PCR was performed for 30 cycles of 94 °C for 30 s, 53 °C for 30 s, and 72 °C for 30 s. The products of the first round of PCR were gel purified and subjected to a second round of PCR using the A1 and A4 primers to generate a product encoding EGFP/csBAFF, which contained the linker sequence (Gly4Ser) 3 between the two domains. Amplification was performed for 30 cycles of denaturation for 45 s at 94 °C, annealing for 30 s at 52 °C, and extension for 90 s at 72 °C (Fig.5 A). The DNA fragment encoding the full-length of cBAFF-R (aa 1–185), was amplified by PCR using the primers P3 and P4 (Table 1). The cBAFF-R and EGFP/csBAFF PCR products were digested with *Nde*I and *Bam*HI or *Nde*I and *Hind*III, respectively, and ligated into the pET-28a plasmid at the corresponding restriction sites. The ligation mixtures were transformed into *Escherichia coli* DH5α competent cells for propagation of the recombinant plasmids. The presence of the pET28a-cBAFF-R and pET28a-EGFP/csBAFF recombinant plasmids was confirmed by restriction endonuclease digestion and sequencing.

The recombinant plasmids pET28a-cBAFF-R and pET28a-EGFP/csBAFF were transformed into competent *E. coli* BL21 (DE3) (Novagen, Darmstadt, Germany) cells to express the fusion protein. Bacteria were cultured in LB medium for kanamycin resistance with vigorous shaking (220 rpm) at 37 °C to an OD600 of ˜ 0.6. To produce soluble cBAFF-R and EGFP/csBAFF proteins, the following induction scheme was established: final isopropyl β-D-1-thiogalactopyranoside (IPTG) concentration, 0.2 mM; induction temperature, 16 °C; total induction duration, 16 h; shaking speed, 100 rpm. After induction, bacteria were harvested by centrifugation at 10,000*g* for 5 min at 4 °C. Pellets were sonicated on ice for a 10 s pulse with an intervening 10 s pause until cells were completely lysed. Lysates were centrifuged at 12,000*g* for 30 min at 4 °C. The supernatants were collected and applied to a nickel column to purify histidine-tagged proteins under native conditions following the manufacturer's instructions. The concentrations of purified csBAFF, EGFP/tsBAFF, and cBAFF-R were determined spectroscopically at 595 nm using a protein assay kit based on the Bradford reagent. Purified fusion proteins were subjected to sodium dodecyl sulfate polyacrylamide gel electrophoresis (SDS-PAGE) using gels containing 12% polyacrylamide. Proteins were detected by staining with Coomassie brilliant blue R-250 or blotted onto nitrocellulose membranes (Amersham, Bucks, UK). Membranes were blocked for 2 h at 37 °C in Tris-buffered saline Tween-20 (TBST) (25 mM Tris − HCl, 125 mM NaCl, 0.1% Tween 20; pH 8.0) containing 5% skim milk. After washing five times with TBS, blots were incubated with an anti-His6-tag monoclonal antibody (Novagen, Darmstadt, Germany) at 37 °C. After washing three times for 5 min with TBST, the membranes were incubated with horseradish peroxidase (HRP)-conjugated goat anti-mouse IgG in TBST containing 5% skim milk for 2 h at 37 °C. After washing, TMB (Promega) was added to promote color development. For all of the purified proteins, the ToxinEraser™ Endotoxin Removal Kit (GenScript, Nanjing, China) was used to remove bacterial endotoxins for subsequent research.

2.9. Measurement of fluorescence spectra

The fluorescence spectra of EGFP/csBAFF and EGFP (5 mM) were determined using an F-2000 fluorescence spectrophotometer (Hitachi, Tokyo, Japan). Emission spectra were measured based on excitation at 488 nm and excitation spectra at 509 nm (Zhang et al., 2010).

2.10. Confocal laser scanning microscopy

Mouse splenic B cells (5×10^5/mL) in staining buffer (PBS with 2% FBS) were incubated for 1 h at 37 °C with/without EGFP/csBAFF (10 mg/mL). Then the cells were washed three times with PBS (pH 7.2). Free EGFP (10 mg/mL) was used as a control. Images were captured using an LSM 510 confocal microscope equipped with a cooled Micro Max CCD camera.

2.11. MTT assay

Purified splenic B cells (adjusted to 10^5/mL) from mice were cultured in RPMI-1640 (Gibco-BRL) containing 10% FCS and 100 U/mL penicillin/streptomycin (Gibco-BRL) in triplicate in 96-well flat-bottomed plates. After 4 h in culture, purified B cells were treated with the indicated concentrations of csBAFF alone or together with a priming agent (SAC; 1:300,000 dilution of stock). Then they were treated with the indicated concentrations of csBAFF or EGFP/csBAFF alone or

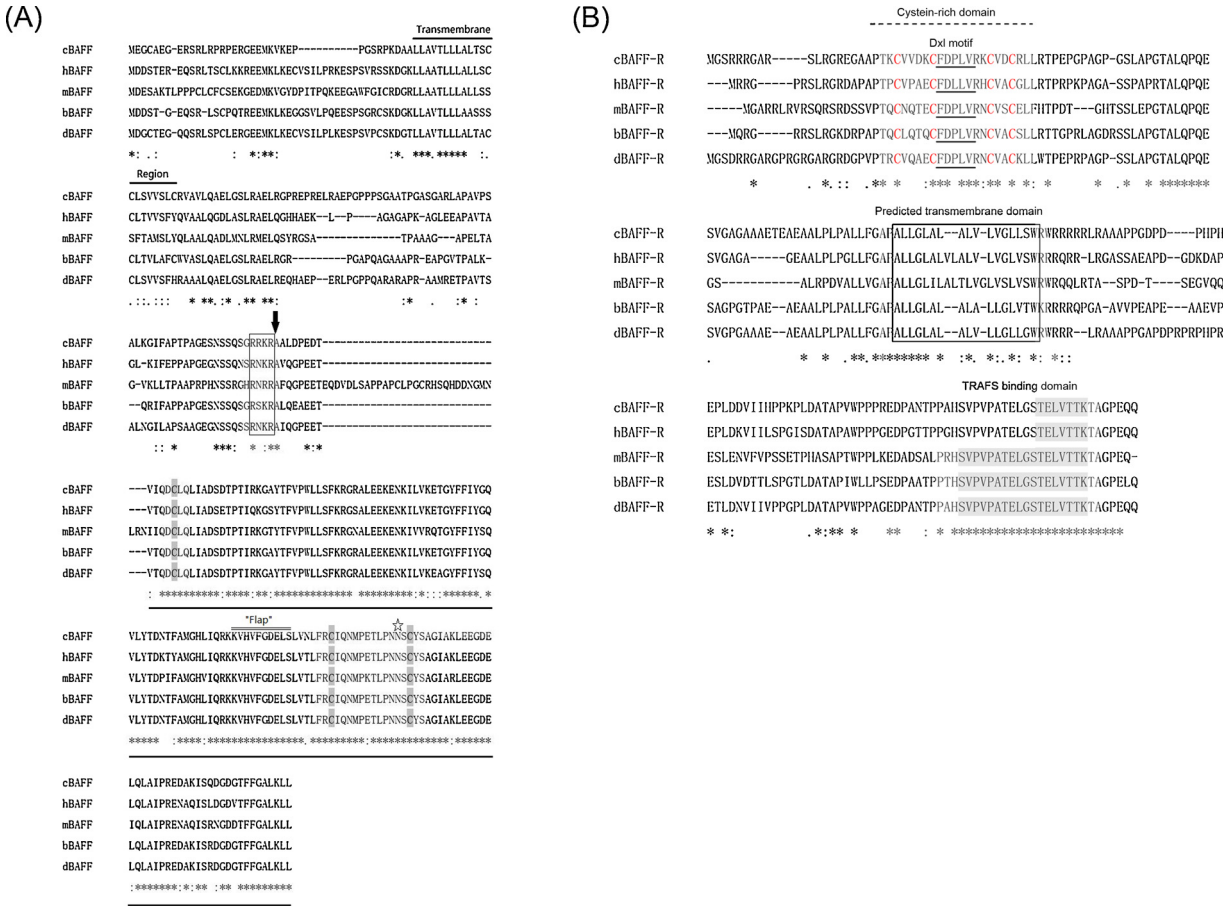

Fig. 2. (A) Alignment of the deduced amino acid sequences of cat BAFF (cBAFF, GenBank Accession No. MH151314), human BAFF (hBAFF, GenBank Accession No.AF116456), murine BAFF (mBAFF, GenBank Accession No. AF119383), bovine BAFF (bBAFF GenBank Accession No. EU213012), and canine BAFF (dBAFF GenBank Accession No. NM_001161710). Multiple alignments were first performed using ClustalW. Asterisks indicate identical residues. Substitutions found to be conservative or semiconservative using ClustalW are marked by colons and periods, respectively. The transmembrane domain is underlined, and the furin cleavage site is boxed and indicated by an arrow. Gray shading indicates three cysteine residues conserved among soluble mature BAFFs. The double line above the BAFF sequences indicates the conserved long D-E loop, known as the flap. The underlined sequence is the conserved TNF domain of BAFF. A conserved potential N-glycosylation site is indicated by a star. **(B)** Alignment of the deduced amino acid sequences of feline, human, mouse, bovine, and dog BAFF-R using ClustalW. Asterisk indicates identical aligned residues. Conservative and semi-conservative substitutions are indicated by a colon and period, respectively.

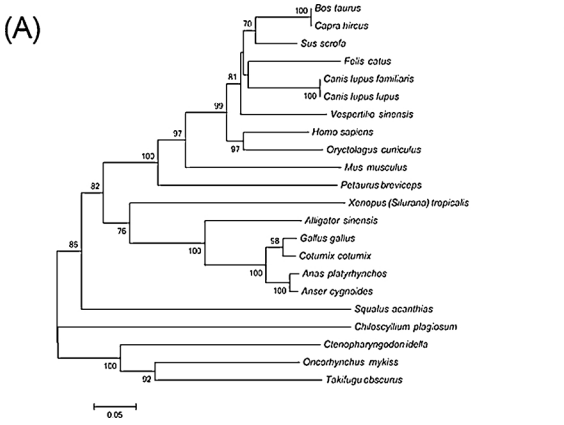

Fig. 3. (A) Phylogenetic tree showing the relationship between the cat BAFF amino acid sequence and other BAFF sequences. The tree was constructed using the neighbor-joining method in ClustalW and MEGA 4.0 and was bootstrapped 1000 times. The GenBank accession numbers of the BAFF proteins are: *Felis catus*, MH151314; *Alligator sinensis*, GU126733; *Gallus gallus*, AF506010; *Anas platyrhynchos*, DQ445092; *Anser cygnoides*, DQ874394; *Bos taurus*, EU213012; *Oryctolagus cuniculus*, EF202603; *Sus scrofa*, DQ872633; *Homo sapiens*, AF116456; *Mus musculus*, AF119383; *Oncorhynchus mykiss*, DQ218467; *Vespertilio sinensis*, JN663829; *Capra hircus*, FJ793192; *Coturnix coturnix*, EU599084; *Petaurus breviceps*, GU377514; *Canis lupus familiaris*, EU909456; *Canis lupus lupus*, NM001161710; *Ctenopharyngodon idella*, KC192768; *Takifugu obscurus*, HQ830264; *Chiloscyllium plagiosum*, HQ893880; *Squalus acanthias*, HE575886; *Xenopus (Silurana) tropicalis*, KC207689. **(B)** Phylogenetic tree showing the relationship between the feline BAFF-R amino acid sequence and that of other BAFF-R proteins. The tree was constructed using the neighbor-joining method in ClustalW and MEGA 4.0 and was bootstrapped 1000 times. The GenBank accession numbers of the BAFF-R proteins are: *Felis catus*, MH244349; *Homo sapiens*, AF373846; *Equus caballus*, JF502272; *Mus musculus*, AF373847; *Gallus gallus*, NM_001037828; *Bos taurus*, NM_001193192; *Canis lupus familiaris*, XM_843968; *Loxodonta Africana*, XM_003419809; *Cricetulus griseus*, XM_003512340; *Cavia porcellus*, XM_003470524; *Nomascus leucogenys*, XM_012507606; *Macaca mulatta*, XM_001101623; *Callithrix jacchus* XM_002763903,; *Rattus norvegicus*, XM_576316; and *Pan troglodytes*, XM_001154286.

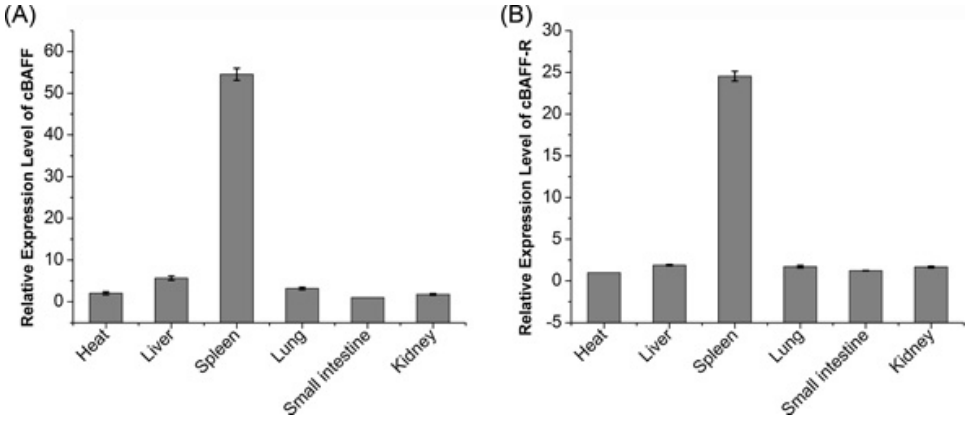

Fig. 4. (A) Mean mRNA levels of the cat BAFF gene by real-time qPCR. Data are $2^{-\Delta\Delta}$Ct levels calculated relative to the tissue with the lowest expression (small intestine) set to 1, normalized to the GAPDH mRNA level. Vertical bars represent means ± SE (n = 3). **(B)** Mean mRNA levels of the cat BAFF-R gene by real-time qPCR. Data are $2^{-\Delta\Delta}$Ct levels calculated relative to the tissue with the lowest expression (heart) set to 1, normalized relative to the GAPDH mRNA level. Vertical bars represent means ± SE.

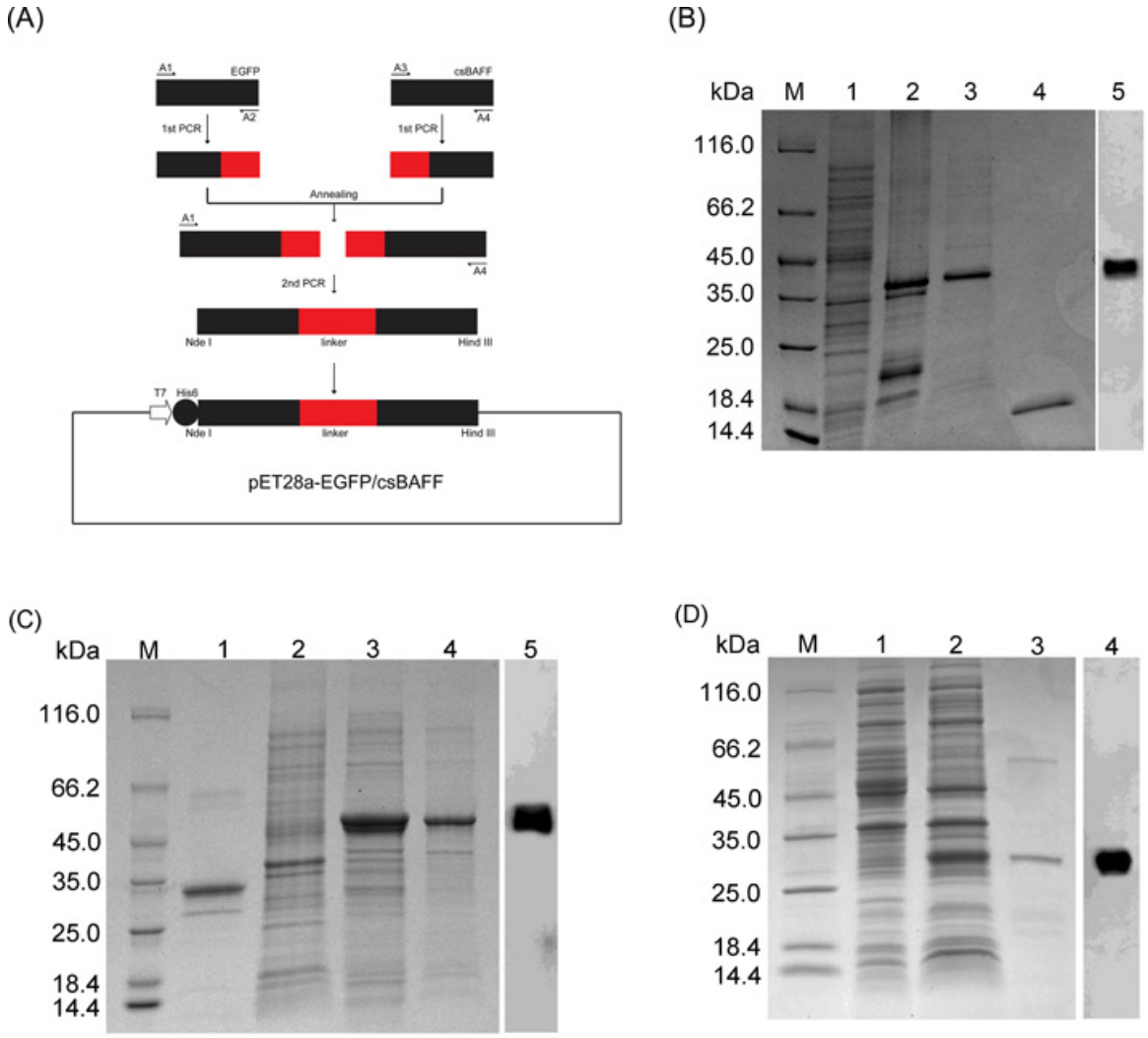

Fig. 5. (A) Schematic representation of the construction of the recombinant vector, pET28a-EGFP/csBAFF. Arrows indicate the primers used. The plasmid pET28a-EGFP/csBAFF contains *Nde*I and *Hind*III ligation sites and encodes a His6-tag fusion protein. T7 and His-tag indicate the T7 promoter and the His6-tag, respectively. SDS-PAGE analyses of recombinant csBAFF, EGFP/csBAFF, and cBAFF-R fusion proteins expressed in *E. coli* BL21 (DE3). Left-most lane, molecular weight marker. (B) Lane 1, lysates of bacteria transformed with empty pSUMO under IPTG induction. Lane 2, lysates of bacteria transformed with pSUMO-csBAFF under IPTG induction. Lane 3, SUMO-csBAFF fusion protein purified by immobilized metal affinity chromatography. Lane 4, purified csBAFF obtained after reloading the digested sample onto the Ni-NTA column. Lane 5, Western blotting of SUMO-csBAFF using an anti-His6 tag mAb. **(C)** Lane 1, EGFP. Lane 2, lysates from bacteria transformed with pET28a-EGFP/csBAFF without IPTG induction. Lane 3, lysates from bacteria transformed with pET28a-EGFP/csBAFF under IPTG induction. Lane 4, EGFP/csBAFF fusion protein purified by immobilized metal affinity chromatography. Lane 5, Western blotting of purified EGFP/csBAFF using an anti-His6 tag mAb. **(D)** Lane 1, lysates from bacteria transformed with empty pET28a and IPTG induction. Lane 2, lysates from bacteria transformed with pET28a-cBAFF-R with IPTG (0.2 mM) induction at 16 °C for 16 h. Lane 3, fusion protein purified by immobilized metal affinity chromatography. Lane 4, Western blotting of cBAFF-R using an anti-His6 tag mAb.

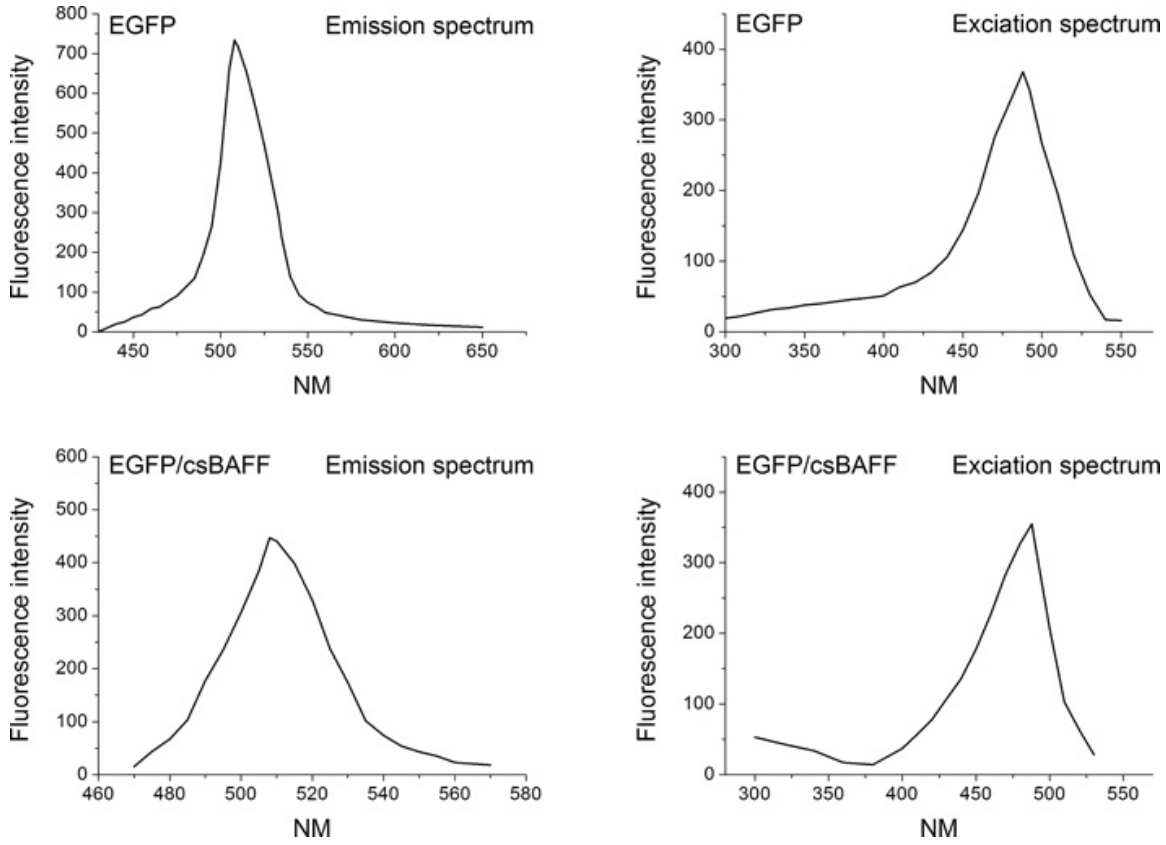

Fig. 6. Fluorescence spectra of free EGFP and EGFP/csBAFF. Emission spectra were measured with excitation at 488 nm over the range 500–600 nm. Excitation spectra were measured with emission at 507 nm over the range 300–500 nm. The maximum emission wavelengths of free EGFP and EGFP/csBAFF were both 507 nm, and the maximum excitation wavelengths were both 488 nm.

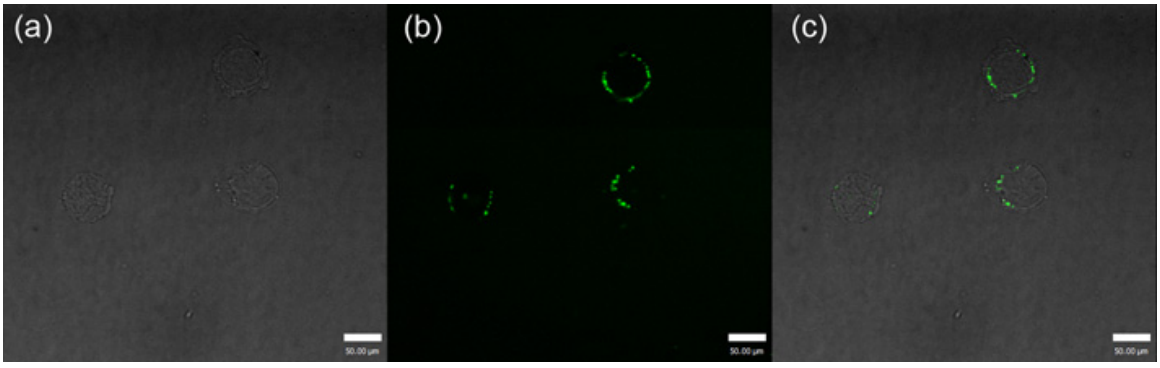

Fig. 7. CLSM images of EGFP/csBAFF bound to mouse splenic B cells. Images were captured using a CCD camera with identical settings below the saturation limits. **(a)** Transmitted light (phase-contrast) image. **(b)** Same images as in **(a)** with EGFP fluorescence (green) following excitation at 488 nm. **(c)** Image merged with **(a)** and **(b)**: B cells not cocultured with EGFP/csBAFF did not yield a signal (data not shown) (see the Web version of the article for interpretation of the colors) (For interpretation of the references to colour in this figure legend, the reader is referred to the web version of this article).

together with 2 mg/mL anti-mouse IgM (Sigma, St. Louis, MO) as a priming agent. msBAFF (10 mg/mL) was used a positive control. PBS alone was added to cells as a control. After incubation at 37 °C in a humidified atmosphere of 5% CO_2 for 48 h, 20 mL 3-(4,5-dimethylthiazol-2-yl)-2,5-diphenyltetrazolium bromide (MTT; 5 mg/mL) was added to each well and allowed to react for 4 h. After centrifugation at 1000 rpm for 10 min, the supernatant (containing medium and unreduced MTT) was carefully removed. Next, 150 mL dimethyl sulfoxide (DMSO) was added to each well to dissolve formazan crystals. Plates were shaken gently for a few minutes until a purple color appeared. OD at 450 nm was measured using an EL_800 Microplate Reader (Bio-Tek Instruments, Inc., Winooski, VT).

2.12. Flow cytometric analyses

Splenic lymphocytes from mice (5×10^6/mL) were cultured for 48 h in medium containing 10 mg/mL csBAFF; PBS was used as a control. Discrimination of dead cells for *in vitro* survival assays was performed *via* staining with propidium iodide (PI; 2.5 mg/mL). Flow cytometric analyses were performed using an FACScan instrument and Cell Quest software (Becton Dickinson, Heidelberg, Germany).

2.13. Affinity determination

The affinity of cBAFF-R for csBAFF was measured *via* surface plasmon resonance (SPR) using a Biacore X100 system. The sensor chip

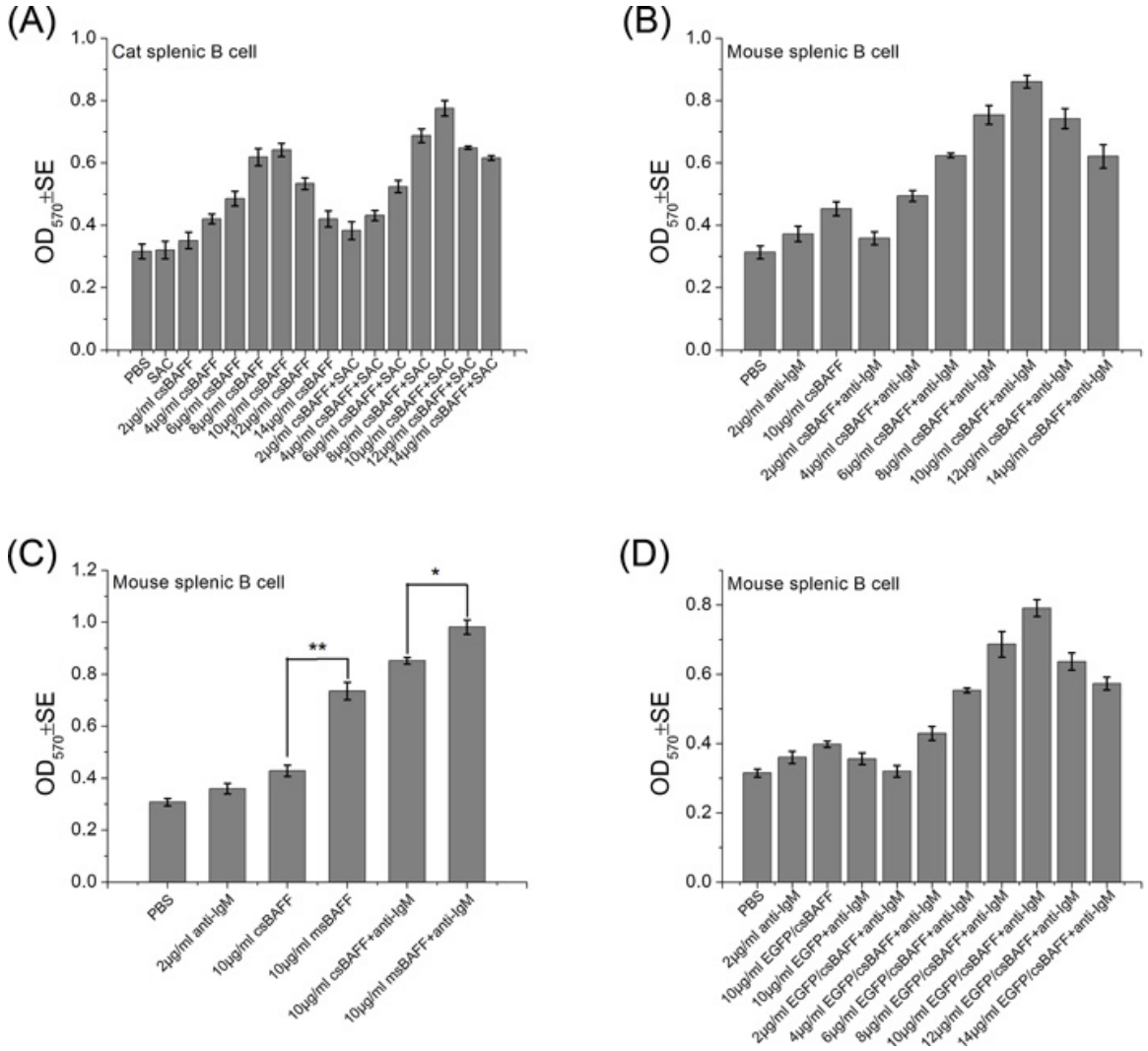

Fig. 8. (A) *In vitro*, csBAFF costimulates the survival of cat splenic B cells in the presence of SAC. Cells cultured with the indicated doses of csBAFF + SAC (1:300,000 dilution of stock) were used as positive controls. Values are means ± SEs. **(B)** csBAFF promotes the survival of mouse splenic B cells in culture. In addition, csBAFF and anti-mouse IgM costimulate thesurvival of mouse B cells *in vitro*. Freshly isolated mouse splenic B cells were cultured with the indicated doses of csBAFF with/without anti-IgM. Anti-IgM was used as the control. Values are means ± SEs of three independent experiments. **(C)** Effects of csBAFF on mouse splenic B-cell survival *in vitro*, compared to msBAFF. Freshly isolated mouse splenic B cells were cultured with/without 2 mg/mL anti-mouse IgM with 10 mg/mL tsBAFF or msBAFF for 72 h and subjected to an MTT assay. Values are means ± SEs. *P < 0.05, **P < 0.01. **(D)** EGFP/csBAFF promotes the survival of mouse splenic B cells in culture. In addition, EGFP/csBAFF and anti-mouse IgM costimulate the survival of mouse B cells *in vitro*. Freshly isolated splenic B cells were cultured with the indicated doses of EGFP/csBAFF with/without anti-IgM. Anti-IgM was used as the control. Values are means ± SEs of three independent experiments.

CM5 was activated by injection of N-hydroxysuccinimide and 1-ethyl-3-(3-diethylaminopropyl) carbodiimide hydrochloride. Next, purified csBAFF (30 μg mL^{-1}) was immobilized on the chip by the standard coupling method at a flow rate of 10 μL·min^{-1} with HBS-EP (10×, pH 7.4, containing 0.1 M N-[2-hydroxyethyl] piperazine-N′-ethanesulfonic acid [HEPES], 1.5 M NaCl, 30 mM ethylenediaminetetraacetic acid [EDTA], and 0.5% [v/v] surfactant P20) as the running buffer. Ethanolamine was injected to block excess reactive groups, and HBS-EP buffer was injected to remove noncovalently bound material. After coupling the chip, cBAFF-R in HBS-EP buffer was injected at a flow rate of 30 μL·min^{-1} for 180 s. Immobilized flow cell 1 was left untreated to serve as a reference surface, and immobilized flow cell 2 was used as the experimental surface. A new injection was performed after injection of 10 mM glycine hydrochloride (pH 1.5) for 30 s (10 μL·min^{-1}) to regenerate the CM5sensor chip, and HBS-EP buffer was injected over the sensor surface for about 100 s. cBAFF-R (12.5, 25, 50, and 100 μg mL^{-1}; 25 μg mL^{-1} was tested in duplicate) and a blank injection were included. Signals from the reference surface were subtracted to correct for nonspecific binding. The corrected results were globally fitted to a 1:1 binding model, and the association rate constant (k_a), dissociation rate constant (k_d), and equilibrium dissociation constant (K_D) were extracted. All data processing and the kinetic curve-fitting procedure were performed with Biacore X100 evaluation software (version 2.0.1).

2.14. Effect of cBAFF-R on B-cell proliferation

B cells proliferate in response to BAFF. We evaluated the inhibitory effects of cBAFF-R on csBAFF-induced B-cell proliferation *in vitro*. Purified B cells from cats were treated with 10 μg mL^{-1} csBAFF and 1, 3, 5, 7, 9, 11, or 13 μg mL^{-1} cBAFF-R. Mouse B cells treated with csBAFF and cBAFF-R were used as the positive control (OD values).

2.15. Structures and molecular docking

The structures of cBAFF and cBAFF-R were predicted using I-TASSER (http://zhanglab.ccmb.med.umich.edu/I-TASSER), an

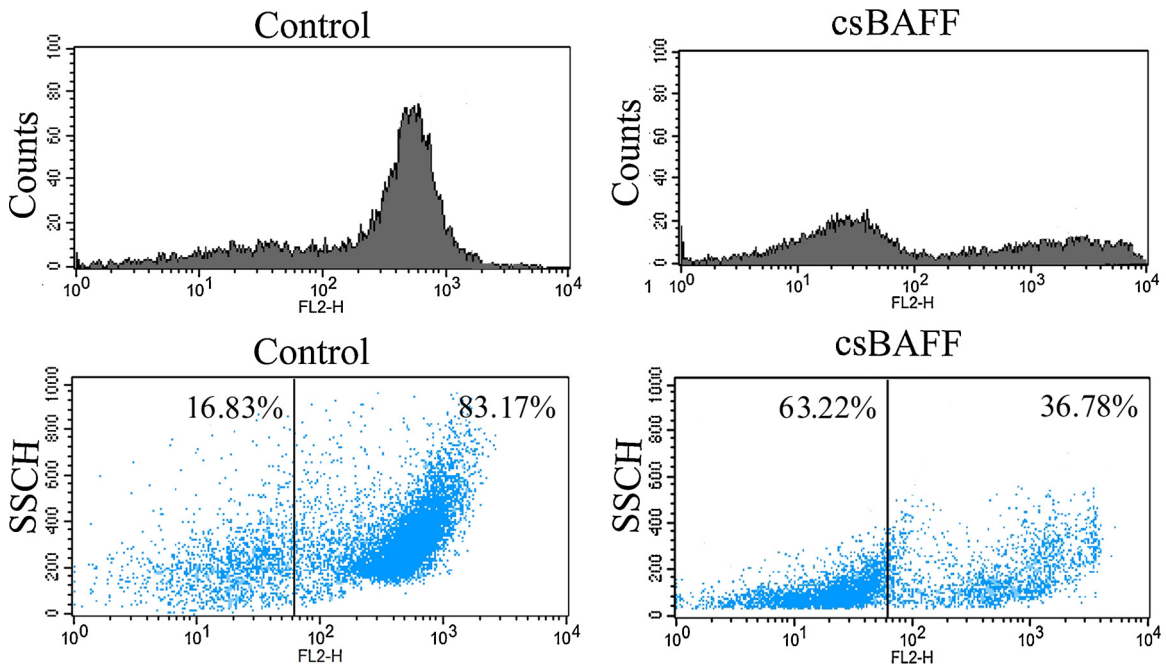

Fig. 9. csBAFF promotes the survival of mouse splenic B cells in culture. Freshly isolated B cells were cultured for 48 h with 10 mg/mL csBAFF or with PBS (control), and analyzed by flow cytometry. To justify the cutoff between live and dead cells by PI staining, the original flow cytometry data including the percentages of dead cells with each treatment are attached.

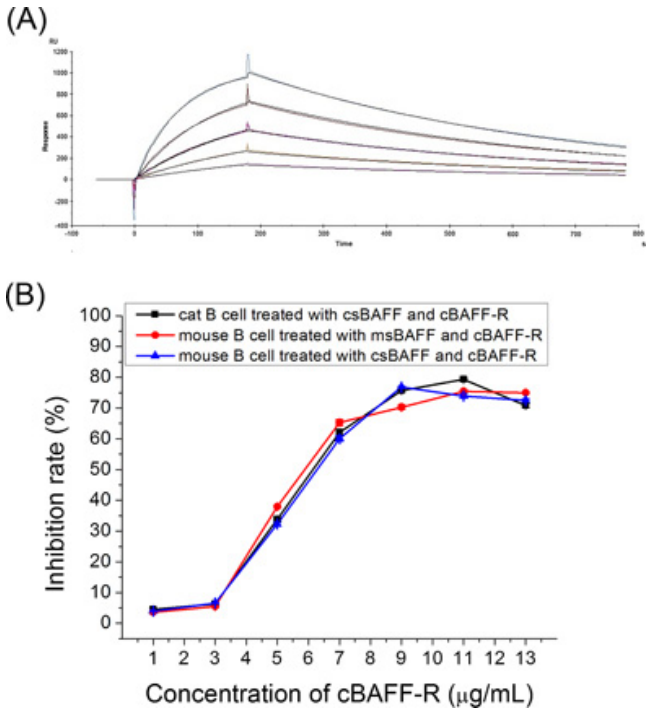

Fig. 10. (A) Sensorgrams and kinetic parameters of the binding between csBAFF and cBAFF-R. **(B)** Binding of cBAFF-R to csBAFF blocked the function of csBAFF *in vitro*. The inhibition rate was determined as: (control – experiment) ÷ (control – blank). Blank, OD value for B cells only; control, cat B cells treated with csBAFF; experimental groups, cat B cells treated with csBAFF and cBAFF-R, mouse B cells treated with msBAFF and cBAFF-R, and mouse B cells treated csBAFF and cBAFF-R. Error bars indicate SE.

Internet-based service for protein structure and function predictions. Three-dimensional (3D) models are built based on multiple-threading alignments using LOMETS and iterative TASSER simulations; then function insights are derived by matching the predicted models with protein function databases. Critical Assessment of Structure Prediction (CASP) experiments were designed to obtain an objective assessment using the state-of-the-art method in the field, and I-TASSER was ranked as the best method in the server section of the recent seventh CASP experiment (Roy et al., 2010; Yang, 2008; Zhang et al., 2017, 2015; Zhang, 2010). To derive the sheet and loop binding conformations, molecular docking was performed using ZDOCK (version 3.0.2) software (Pierce et al., 2011). Implementing a fast Fourier transform (FFT)-based initial-stage rigid-body molecular docking algorithm (Chen and Weng, 2010), ZDOCK performs a global search in the translational and rotational space to produce all possible binding configurations between proteins. With a composite scoring function that combines pairwise shape complementarity with desolvation and electrostatics, the performance of ZDOCK in critical assessment of prediction of interaction (CAPRI) challenge proves that it is among the best protein–protein docking algorithms (Chen et al., 2010a, b). ZDOCK created 3600 and retained 2000 putative sheet and loop binding configurations, and the complexes showing the top default ZDOCK scores were considered the most likely binding configurations. To remove bad atomic contacts around the binding interface, each binding complex was subjected to 2000-step steepest descent and 2,000step conjugate gradient energy minimizations using the SANDER module in AMBER 12 software (Case et al., 2010).

2.16. Statistical analyses

All statistical tests were performed in triplicate. Data are means ± standard error (SEs) Statistical analyses were performed using Student's *t*-test (Statistica; StatSoft Inc., Tulsa, OK). The significance of differences was evaluated by one-way analysis of variance (ANOVA); $P < 0.05$ was taken to indicate statistical significance.

3. Results

3.1. Identification of the full-length cBAFF and cBAFF-R cDNA

A 530 bp cDNA fragment with high sequence similarity to

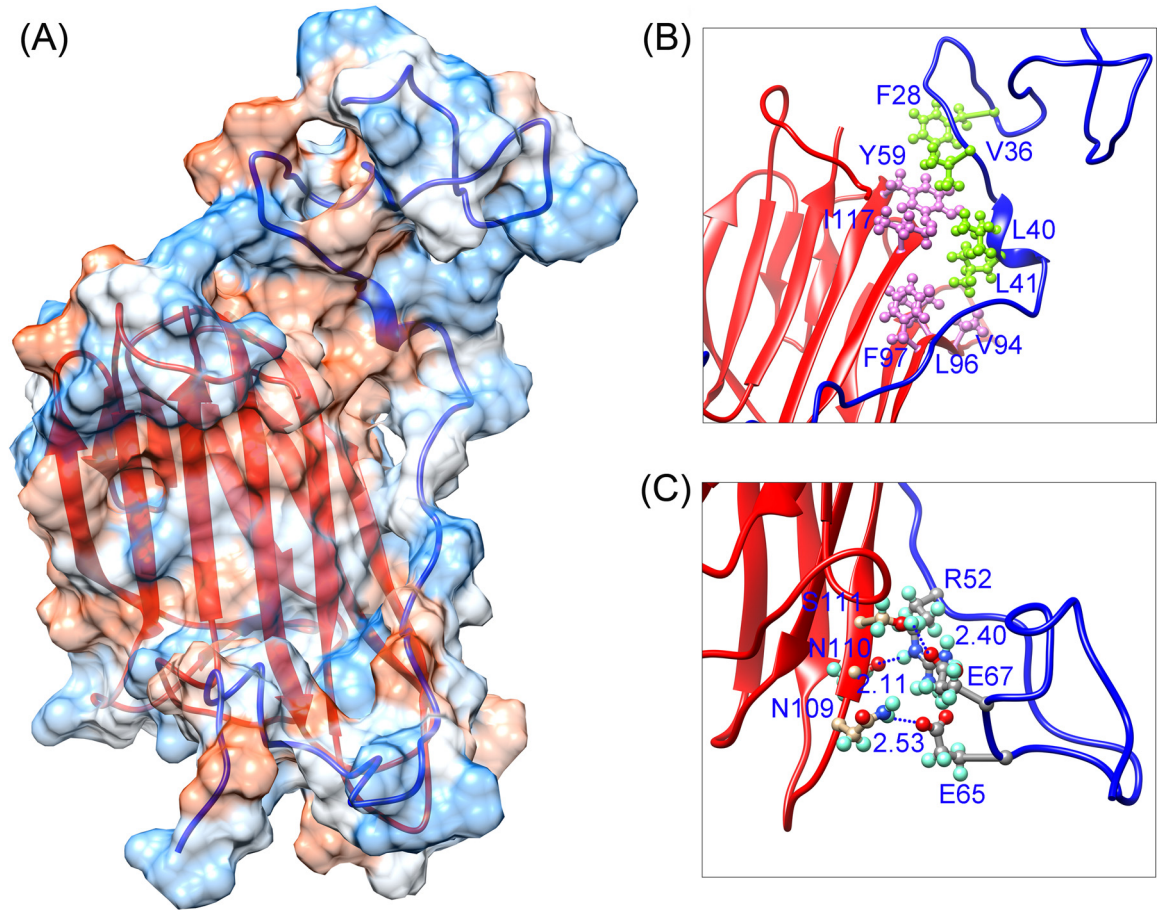

Fig. 11. (A) Schematic representation of the csBAFF/cBAFF-R complex. **(B)** Hydrophobic interactions between csBAFF and the DxL motif of the cBAFF-R CRD-binding domain. **(C)** Three intermolecular hydrogen bonds in the csBAFF/cBAFF-R complex.

mammalian BAFF was obtained by RT-PCR using the primers cBAFF-1 and cBAFF-2. A 342 bp fragment from 5′RACE and a 657 bp fragment from 3′RACE were also obtained. The full-length cDNA (1529 bp) of cBAFF was amplified by PCR and deposited into GenBank under accession number MH151314. This open reading frame (ORF) encoded a protein of 285 amino acids with a 152 aa mature peptide. The molecular weight of csBAFF was approximately 17.08 kDa, and its isoelectric point was 4.814. The nucleotide and predicted amino acid sequences of the full-length cDNA are shown in Fig. 1A. The ORF 558 bp coding sequence of cBAFF-R was obtained by RT-PCR amplification and deposited into GenBank under accession number MH244349. This ORF encoded a protein of 185 amino acids. The molecular weight of cBAFF-R was approximately 21.592 kDa, and the isoelectric point was 8.726. The cDNA sequence of cBAFF-R and the deduced amino acid sequence are shown in Fig. 1B.

3.2. Sequence comparison and phylogenetic analyses

BLAST searches indicated sequence identities of 88.9%, 67.9%, 94.1%, and 93.5% at the amino-acid level between csBAFF and hsBAFF, E. msBAFF, bsBAFF, and dsBAFF, respectively, markedly higher than those for most other known cytokines. The similarities at the amino acid level between cBAFF-R and hBAFF-R, E. mBAFF-R, bBAFF-R, and dBAFF-R were 49.2%, 41.9%, 47.6%, and 55.2%, respectively, markedly higher than those for most other known cytokines. BAFF and BAFF-R multiple alignments are shown in Fig. 2. A phylogenetic tree constructed using the full-length amino acid sequences of BAFF and BAFF-R showed that csBAFF and cBAFF-R cluster together with mammalian sequences and away from other vertebrate BAFF and BAFF-R proteins (Fig. 3).

3.3. Tissue-specific expression of cBAFF and cBAFF-R

SYBR Green I (Sigma–Aldrich, St. Louis, MO) qPCR analyses revealed that the cBAFF gene was expressed in all tissues examined, with the highest expression in the spleen, followed by the liver, lung, kidney, heart, and small intestine (Fig. 4A). The cBAFF-R gene was expressed in all tissues examined, with the highest expression in the spleen, followed by the liver, lung, kidney, small intestine, and heart (Fig. 4B). These results indicate that BAFF and BAFF-R play an important role in the feline immune system.

3.4. Expression, purification, and enzymolysis of SUMO-csBAFF

To test the bioactivity of csBAFF, recombinant SUMO-csBAFF was produced in *Escherichia coli*. The pSUMO-His6-csBAFF plasmids were transformed into *E. coli* BL21(DE3), and the SUMO-His6-tagged csBAFF was expressed and purified under the optimal conditions. SDS-PAGE after IPTG induction showed a band at approximately 37.5 kDa, corresponding to the expected size of the fusion protein, which was absent in BL21(DE3) transformed with empty pSUMO (Fig. 5B, lanes 1 and 2). After one-step purification of the soluble fusion protein, the yield of eluted soluble proteins, with a purity of ≥90%, was about 1 mg/mL (Fig. 5B, lane 3) as assessed by the Bradford method. As shown in Fig. 5B (lane 4), after dialysis and cleavage by the SUMO-specific protease Ulp1, the fusion protein released a 20 kDa fragment (SUMO dimer) and soluble csBAFF (17.5 kDa). After His-Bind column purification, the vast majority of undigested SUMO-csBAFF and SUMO

with N-terminal His-tags remained bound to the column. The expressed SUMO-csBAFF was recognized by a mouse anti-His6-tag monoclonal antibody (Fig. 5B, lane 5).

3.5. In vitro expression and purification of EGFP/csBAFF and cBAFF-R proteins

For EGFP/tsBAFF and cBAFF-R protein expression, pET28a-EGFP/tsBAFF and pET28a-cBAFF-R plasmids were transformed into *E. coli* BL21 (DE3). The His6-tagged EGFP/csBAFF (46.236 kDa) and cBAFF-R (27.734 kDa) were expressed and purified under the optimal conditions. Soluble recombinant proteins were purified using Ni-nitrilotriacetic acid resin. After IPTG induction, the SDS-PAGE bands of 46.236 kDa (Fig. 5C, lane 3) and 27.734 kDa (Fig. 5D, lane 2) were consistent with the expected sizes of the respective fusion products. The identities of the purified proteins were determined using an anti-His6 monoclonal antibody (Novagen, Darmstadt, Germany). In Western blotting analyses, the recombinant proteins yielded bands with estimated molecular weights of 46.236 kDa (Fig. 5C, lane 5) and 27.734 kDa (Fig. 5D, lane 4). The purified EGFP/csBAFF and cBAFF-R proteins were passed through a 0.22 μm filter and stored at 80 °C until needed.

3.6. Fluorescence activity

When enhanced green fluorescent protein (EGFP) is fused to the N-terminus of overexpressed globular proteins, overexpression in soluble form allows EGFP to fold correctly. To confirm correct folding of the EGFP domain, the fluorescence of purified soluble EGFP/csBAFF was examined. The fluorescence properties of EGFP/csBAFF were similar to those of free EGFP, with an excitation maximum at 488 nm and emission maximum at 508 nm. However, the fluorescence intensity was weaker than that of free EGFP (Fig. 6). These observations indicate that the excitation or emission spectrum of the EGFP/csBAFF fusion protein did not shift compared to free EGFP. The decreased fluorescence of the chimera may be explained by quenching by csBAFF.

3.7. Recombinant EGFP/csBAFF binds to the surface of mouse splenic B cells

BAFF can bind to three receptors of the TNF receptor family: TACI, BCMA, and BAFF-R. TACI is expressed on B cells and activated T cells, whereas BAFF-R and BCMA are expressed mainly or exclusively on B cells (JS et al., 2001). The major BAFF receptor, BAFF-R, is present in the nucleus in addition to the plasma membrane and cytoplasm (Fu et al., 2009). The binding activity of EGFP/csBAFF was confirmed by confocal laser scanning microscopy (CLSM) using mouse splenic lymphocytes (Fig. 7). CBAFF bound to its major receptor (BAFF-R) mainly in the nucleus and cytoplasm of B cells, consistent with recent research. EGFP or csBAFF protein was used as the negative control.

3.8. csBAFF and EGFP/csBAFF promote B-cell survival

In vitro, human sBAFF costimulates B-cell proliferation in response to anti-IgM as a priming agent, and so csBAFF may have similar bioactivity. Freshly purified splenic B cells from cats were costimulated with purified csBAFF proteins at the indicated concentrations together with the priming agent SAC (1:300,000 dilution of stock) and subjected to MTT assay. csBAFF demonstrated strong, saturable costimulation of B cell survival (Fig. 8A). The proliferation of B cells was entirely dependent on the presence of the priming agent, SAC, which indicates that csBAFF also functions as a costimulator of B-cell survival (Fig. 8A). Splenic B cells from mice were cultured with varying concentrations of csBAFF together with the priming agent, anti-mouse IgM, for 48 h; this resulted in a dose-dependent response (Fig. 8B). The viability of B cells in cultures treated with 6–12 μg/mL csBAFF was one- to two-fold higher than that of those in control cultures with PBS, while that in cultures costimulated with csBAFF and anti-IgM at the same dose was twofold that in cultures stimulated with anti-IgM, and higher than that in the culture treated with csBAFF alone. Anti-IgM (negative control) did not promote the survival of B cells. As shown in Fig. 8C, 10 μg/mL msBAFF significantly stimulated mouse splenic B-cell survival compared to 10 μg/mL csBAFF with or without anti-mouse IgM ($P < 0.01$ for treatment with csBAFF or msBAFF alone and $P < 0.05$ for csBAFF or msBAFF together with anti-mouse IgM). EGFP/csBAFF promoted the survival of B cells alone and in conjunction with anti-IgM, similar to the effects of csBAFF (Fig. 8D). The optimal concentration of EGFP/csBAFF for stimulating B-cell survival was 10 μg/mL. Flow cytometric analyses showed that, after 48 h, although cells rapidly died, csBAFF markedly prolonged the survival of splenic B cells in culture (Fig. 9).

These results show that csBAFF promotes the survival of mouse splenic B cells in a manner in part dependent on the presence of anti-IgM. Therefore, csBAFF functions as a costimulator of B-cell survival, similar to human sBAFF.

3.9. Affinity determination and blocking of B-cell survival by cBAFF-R in vitro

Kinetic analyses were performed to determine the affinity of cBAFF-R for csBAFF. Sensorgrams of cBAFF-R against csBAFF are shown in Fig. 10A; all of the data obtained could be used in further kinetic analyses, which indicates high accuracy and good repeatability. Kinetic analyses showed that cBAFF-R bound to csBAFF (K_D 7.638×10^{-7} M).

Costimulation with His6-sBAFF maintained the survival of B cells *in vitro*. However, the addition of cBAFF-R suppressed the function of sBAFF (Fig. 11B), which indicates that cBAFF-R binds to csBAFF and msBAFF. In addition, this blocking effect was slightly higher than that of cat B cells treated with csBAFF and cBAFF-R and of mouse B cells treated with msBAFF and cBAFF-R. Therefore, the interaction between BAFF-R and BAFF is evolutionarily conserved.

3.10. Binding conformation

The binding conformation of csBAFF and cBAFF-R is shown in Fig. 11. From the hydrophobic surface of binding complex of csBAFF and cBAFF-R (blue and orange indicate hydrophilic and hydrophobic regions, respectively), we identified two regions that closely interacted at the interface, *i.e.*, the orange hydrophobic region (upper part) and the blue hydrophilic region (lower part) (Fig. 11A). Further analyses revealed that the hydrophobic interactions mainly occurred between the Y59, I117, F97, L96, and V94 residues of csBAFF and the F28, V36, L40, and L41 residues of the cBAFF-R Dxl motif (Fig. 11B). These nonpolar residues form close contacts *via* van der Waals interactions. The three intermolecular hydrogen bonds between csBAFF and cBAFF-R are shown in Fig. 11C. The atoms involved in the $N–H_{N109}\cdots O_{E65}$, $N–H_{R52}\cdots O_{N110}$, and $O–H_{S111}\cdots O_{E67}$ hydrogen bonds were in the proper positions and the bond lengths were 2.53, 2.11, and 2.40 Å, respectively, which indicates stable hydrogen bonding. Therefore, hydrophobic interactions and hydrogen bonds mediate the binding of csBAFF and cBAFF-R.

4. Discussion

BAFF is a potent survival factor for B cells and plays a central role in B-cell maturation and survival, as well as in T-cell activation. There is increasing evidence that BAFF influences many important biological traits, including immune recognition and susceptibility to autoimmune diseases. Therefore, the BAFF gene is a good candidate for evolutionary studies and investigations of vertebrate immune mechanisms.

BAFF receptors are different from most TNF receptors. For example, BAFF-R, TACI, and BCMA lack a signal peptide and death domain; the latter suggests that their functions are irrelevant to apoptosis. In

addition, most TNF receptors are organized into multiple CRDs, each comprising six cysteine residues and three disulfide bonds (Smith et al., 1994). However, the CRD of BAFF-R contains only four cysteine residues and two disulfide bonds, which makes it the smallest CRD in the TNF receptor family.

We identified and characterized the cat homologs of BAFF and BAFF-R. The cloning strategy was based on the nucleotide sequence homology between the cat and other species (human, mouse, bovine, and dog). The cBAFF protein contains a predicted transmembrane domain and a putative furin protease cleavage site, similar to other mammalian BAFFs. The cladogram indicated that csBAFF showed high homology with other BAFFs. Similar to other BAFF-Rs, the extracellular and cytoplasmic domains of cBAFF-R contain one CRD and a TRAF3-binding domain, which are more conserved than the other BAFF-R regions. The DxL motif located in the CRD plays an important role in the BAFF–BAFF-R interaction (Kim et al., 2003), and the TRAF3-binding domain is associated with the NF-κB signaling pathway (Kim et al., 2003). cBAFF-R also showed high homology with other BAFF-Rs. csBAFF and cBAFF-R mRNA were expressed in various tissues, particularly in the lymphatic organs, such as the spleen, which is rich in B lymphocytes. These results indicate that the functions of cBAFF and BAFF-R in immunity are similar to those of their homologs in other mammalian species.

Recombinant csBAFF, EGFP/ csBAFF, and cBAFF-R were expressed and purified *in vitro*. csBAFF and SAC costimulated the proliferation of cat B cells in a dose-dependent manner, and csBAFF and anti-mouse IgM costimulated the survival of mouse B cells in a dose-dependent manner (Figs. 8A, 9B). EGFP/csBAFF had similar effects. These findings correspond well with a recent report that the BAFF–BAFF-R interaction is indispensable for Bcell survival and maturation in the spleen (Batten et al., 2000). The proliferation induced by BAFF is a consequence of more cells surviving to enter the cell cycle, rather than the actual costimulation of B cells (Do et al., 2000). Generally, BAFF specifically binds to BAFF-R. To examine receptor-binding activity, we constructed an EGFP–csBAFF fusion protein; EGFP/csBAFF not only bound to receptor-positive cells but also costimulated the proliferation of B cells *in vitro*. Moreover, cBAFF-R was expressed and purified. In the BAFF–-BAFF-R complex, the BAFF-R extracellular domain has a DxL motif that binds to a shallow hydrophobic pocket of sBAFF. Because the surface area for the interaction is relatively small, the BAFF–BAFF-R interaction could be a therapeutic target for BAFF-mediated diseases. Affinity determination showed that cBAFF-R bound to csBAFF, with a K_D value of 7.638×10^{-7} M. The duration of binding was around 180 s, after which the two proteins began to dissociate. In addition, recombinant cBAFF-R blocked the function of sBAFF *in vitro*.

In summary, we successfully cloned and characterized the cBAFF and BAFF-R genes. We also analyzed the structures and bioactivities of, and the interactions between, cBAFF and BAFF-R.

Our results suggest that csBAFF plays an important role in the survival of cat B cells, and has functional cross-reactivity with homologs in other mammalian species. These results will facilitate immune-modulating experiments with vaccination strategies in cats. The functional cross-reactivity between human and cBAFF is likely due to its high degree of evolutionary conservation, which suggests the utility of BAFF as a model of human diseases. Our findings will enable further investigation of the role of the BAFF–BAFF-R system in regulating B-cell survival, as well as B-cell–related immune diseases, in cats.

Conflicts of interest

The authors declare no conflicts of interest.

Acknowledgments

This work was supported by research start-up funding from Nanjing Normal University (184080H202B152), the National Science Foundation of China (No. 30271093), Natural Science Foundation of China (No. 81501204), and The Research Fund for the Doctoral Program of Higher Education (No. 200803160002). The project was also funded by the Priority Academic Program Development of Jiangsu Higher Education Institutions (PAPD).

References

Avery, D.T., Kalled, S.L., Ellyard, J.I., Ambrose, C., Bixler, S.A., Thien, M., Brink, R., Mackay, F., Hodgkin, P.D., Tangye, S.G., 2003. BAFF selectively enhances the survival of plasmablasts generated from human memory B cells. J. Clin. Invest. 112, 286–297.

Batten, M., Groom, J., Cachero, T.G., Qian, F., Schneider, P., Tschopp, J., Browning, J.L., Mackay, F., 2000. Baff mediates survival of peripheral immature B lymphocytes. J. Exp. Med. 192, 1453–1466.

Bodmer, J.L., Schneider, P., Tschopp, J., 2002. The molecular architecture of the TNF superfamily. Trends Biochem. Sci. 27, 19–26.

Bossen, C., Schneider, P., 2006. BAFF, APRIL and their receptors: structure, function and signaling. Semin. Immunol. 18, 263–275.

Case, D.A., Cheatham, T.E., Darden, T., Gohlke, H., Luo, R., Merz, K.M., Onufriev, A., Simmerling, C., Wang, B., Woods, R.J., 2010. The Amber biomolecular simulation programs. J. Comput. Chem. 26, 1668–1688.

Chen, R., Weng, Z., 2010. Docking unbound proteins using shape complementarity, desolvation, and electrostatics. Proteins Struct. Funct. Bioinform. 47, 281–294.

Chen, R., Li, L., Weng, Z., 2010a. ZDOCK: an initial-stage protein-docking algorithm. Proteins-structure Function & Bioinformatics 52, 80–87.

Chen, R., Tong, W., Mintseris, J., Li, L., Weng, Z., 2010b. ZDOCK predictions for the CAPRI challenge. Proteins-structure Function & Bioinformatics 52, 68–73.

Darce, J.R., Arendt, B.K., Xiaosheng, W., Jelinek, D.F., 2007. Regulated expression of BAFF-binding receptors during human B cell differentiation. J. Immunol. 179, 7276–7286.

Do, R.K.G., Eunice, H., Hayyoung, L., Tourigny, M.R., David, H., Selina, C.K., 2000. Attenuation of apoptosis underlies B lymphocyte stimulator enhancement of humoral immune response. J. Exp. Med. 192, 953–964.

Fu, L., Lin-Lee, Y.C., Pham, L.V., Tamayo, A.T., Yoshimura, L.C., Ford, R.J., 2009. BAFF-R promotes cell proliferation and survival through interaction with IKKbeta and NF-kappaB/c-Rel in the nucleus of normal and neoplastic B-lymphoid cells. Blood 113, 4627–4636.

Gross, J.A., Johnston, J., Mudri, S., Enselman, R., Dillon, S.R., Madden, K., Xu, W., Parrish-Novak, J., Foster, D., Lofton-Day, C., Moore, M., Littau, A., Grossman, A., Haugen, H., Foley, K., Blumberg, H., Harrison, K., Kindsvogel, W., Clegg, C.H., 2000. TACI and BCMA are receptors for a TNF homologue implicated in B-cell autoimmune disease. Nature 404, 995–999.

Guan, N.L., Sutherland, A.P.R., Rebecca, N., Fang, Q., Cachero, T.G., Scott, M.L., Thompson, J.S., Julie, W., Tatyana, C., Joanna, G., 2004. B cell-activating factor belonging to the TNF family (BAFF)-R is the principal BAFF receptor facilitating BAFF costimulation of circulating T and B cells. J. Immunol. 173, 807–817.

Karpusas, M., Cachero, T.G., Qian, F., Boriack-Sjodin, A., Mullen, C., Strauch, K., Hsu, Y.M., Kalled, S.L., 2002. Crystal structure of extracellular human BAFF, a TNF family member that stimulates B lymphocytes 1. J. Mol. Biol. 315, 1145–1154.

Khare, S.D., Sarosi, I., Xia, X.Z., Mccabe, S., Miner, K., Solovyev, I., Hawkins, N., Kelley, M., Chang, D., Van, G., 2000. Severe B cell hyperplasia and autoimmune disease in TALL-1 transgenic mice. Proc. Natl. Acad. Sci. U.S.A. 97, 3370–3375.

Kim, H.M., Yu, K.S., Lee, M.E., Shin, D.R., Kim, Y.S., Paik, S.G., Yoo, O.J., Lee, H., Lee, J.O., 2003. Crystal structure of the BAFF-BAFF-R complex and its implications for receptor activation. Nat. Struct. Biol. 10, 342.

Kowalczyk-Quintas, C., Chevalley, D., Willen, L., Jandus, C., Vigolo, M., Schneider, P., 2018. Inhibition of membrane-bound BAFF by the Anti-BAFF antibody belimumab. Front. Immunol. 9, 2698.

Lilian, I., Reyes, S., Francisca, L.B.M., Fernanda, R.V., Patricia, G.J., Rodrigo, N.P., 2006. [BAFF: a regulatory cytokine of B lymphocytes involved in autoimmunity and lymphoid cancer]. Rev. Mã©dica Chile 134, 1175–1184.

Liu, Y., Xu, L., Opalka, N., Kappler, J., Shu, H.B., Zhang, G., 2002. Crystal structure of sTALL-1 reveals a virus-like assembly of TNF family ligands. Cell 108, 383–394.

Mackay, F., Ambrose, C., 2003. The TNF family members BAFF and APRIL: the growing complexity. Cytokine Growth Factor Rev. 14, 311–324.

Mackay, F., Leung, H., 2006. The role of the BAFF/APRIL system on T cell function. Semin. Immunol. 18, 284–289.

Mackay, F., Schneider, P., 2009. Cracking the BAFF code. Nat. Rev. Immunol. 9, 491–502.

Mackay, F., Woodcock, S.A., Lawton, P., Ambrose, C., Baetscher, M., Schneider, P., Tschopp, J., Browning, J.L., 1999. Mice transgenic for baff develop lymphocytic disorders along with autoimmune manifestations. J. Exp. Med. 190, 1697–1710.

Mackay, F., Silveira, P.A., Brink, R., 2007. B cells and the BAFF/APRIL axis: fast-forward on autoimmunity and signaling. Curr. Opin. Immunol. 19, 327–336.

Marsters, S.A., Yan, M., Pitti, R.M., Haas, P.E., Dixit, V.M., Ashkenazi, A., 2000. Interaction of the TNF homologues BLyS and APRIL with the TNF receptor homologues BCMA and TACI. Curr. Biol. 10, 785–788.

Mihalcik, S.A., Tschumper, R.C., Jelinek, D.F., 2010. Transcriptional and post-transcriptional mechanisms of BAFF-receptor dysregulation in human B lineage malignancies. Cell Cycle 9, 4884–4892.

Moore, P.A., Belvedere, O., Orr, A., Pieri, K., Lafleur, D.W., Feng, P., Soppet, D., Charters, M., Gentz, R., Parmelee, D., 1999. BLyS: member of the tumor necrosis factor family and B lymphocyte stimulator. Science 285, 260–263.

Mukhopadhyay, A., Ni, J., Zhai, Y., Yu, G.L., Aggarwal, B.B., 1999. Identification and characterization of a novel cytokine, THANK, aTNF homologue that ActivatesApoptosis, nuclear Factor-魏B, and c-Jun NH2-Terminal kinase. J. Biol. Chem.
Nakamura, N., Hase, H., Sakurai, D., Yoshida, S., Abe, M., Tsukada, N., Takizawa, J., Aoki, S., Kojima, M., Nakamura, S., 2005. Expression of BAFF-R (BR3) in normal and neoplastic lymphoid tissues characterized with a newly developed monoclonal antibody. Virchows Arch. 447, 53–60.
Ng, L.G., Mackay, C.R., Mackay, F., 2005. The BAFF/APRIL system: life beyond B lymphocytes. Mol. Immunol. 42, 763–772.
Parameswaran, R., Müschen, M., Kim, Y.M., Groffen, J., Heisterkamp, N., 2010. A functional receptor for B-cell-activating factor is expressed on human acute lymphoblastic leukemias. Cancer Res. 70, 4346–4356.
Pierce, B.G., Hourai, Y., Weng, Z., 2011. Accelerating protein docking in ZDOCK using an advanced 3D convolution library. PLoS One 6, e24657.
Rahman, Z.S., Rao, S.P., Kalled, S.L., Manser, T., 2003. Normal induction but attenuated progression of germinal center responses in BAFF and BAFF-R signaling–Deficient mice. J. Exp. Med. 198, 1157–1169.
Rolink, A.G., Tschopp, J., Schneider, P., Melchers, F., 2015. BAFF is a survival and maturation factor for mouse B cells. Eur. J. Immunol. 32, 2004–2010.
Roy, A., Kucukural, A., Zhang, Y., 2010. I-TASSER: a unified platform for automated protein structure and function prediction. Nat. Protoc. 5, 725.
Schiemann, B., Gommerman, J.L., Vora, K., Cachero, T.G., Shulgamorskaya, S., Dobles, M., Frew, E., Scott, M.L., 2001. An essential role for BAFF in the normal development of B cells through a BCMA-independent pathway. Science 293, 2111–2114.
Schmidt, H.A., Strimmer, K., Vingron, M., Von, H.A., 2002. TREE-PUZZLE: maximum likelihood phylogenetic analysis using quartets and parallel computing. Bioinformatics 502–504.
Schneider, P., Mackay, F., Steiner, V., Hofmann, K., Bodmer, J.L., Holler, N., Ambrose, C., Lawton, P., Bixler, S., Achaorbea, H., 1999. BAFF, a novel ligand of the tumor necrosis factor family, stimulates B cell growth. J. Exp. Med. 189, 1747–1756.
Shu, H.B., Johnson, H., 2000. B cell maturation protein is a receptor for the tumor necrosis factor family member TALL-1. Proc. Natl. Acad. Sci. U.S.A. 97, 9156–9161.
Shu, H.B., Hu, W.H., Johnson, H., 1999. TALL-1 is a novel member of the TNF family that is down-regulated by mitogens. J. Leukoc. Biol. 65, 680–683.
Smith, C.A., Farrah, T., Goodwin, R.G., 1994. The TNF receptor superfamily of cellular and viral proteins: activation, costimulation, and death. Cell 76, 959.
Sutherland, A.P., Mackay, F., Mackay, C.R., 2006. Targeting BAFF: immunomodulation for autoimmune diseases and lymphomas. Pharmacol. Ther. 112, 774–786.
Tangye, S.G., Bryant, V.L., Cuss, A.K., Good, K.L., 2006. BAFF, APRIL and human B cell disorders. Semin. Immunol. 18, 305–317.
Tedder, T.F., 2009. CD19: a promising B cell target for rheumatoid arthritis. Nat. Rev. Rheumatol. 5, 572.
Thompson, J.S., Schneider, P., Kalled, S.L., Wang, L., Lefevre, E.A., Cachero, T.G., Mackay, F., Bixler, S.A., Zafari, M., Liu, Z.Y., 2000. BAFF binds to the tumor necrosis factor receptor-like molecule B cell maturation antigen and is important for maintaining the peripheral B cell population. J. Exp. Med. 192, 129–136.
Thompson, J.S., Bixler, S.A., Qian, F., Vora, K., Scott, M.L., Cachero, T.G., Hession, C., Schneider, P., Sizing, I.D., Mullen, C., 2001. BAFF-R, a newly identified TNF receptor that specifically interacts with BAFF. Science 293, 2108–2111.
Tribouley, C., Wallroth, M., Chan, V., Paliard, X., Fang, E., Lamson, G., Pot, D., Escobedo, J., Williams, L.T., 1999. Characterization of a new member of the TNF family expressed on antigen presenting cells. Biol. Chem. 380, 1443–1447.
Vallabhapurapu, S., Matsuzawa, A., Zhang, W., Tseng, P.H., Keats, J.J., Wang, H., Vignali, D.A., Bergsagel, P.L., Karin, M., 2008. Nonredundant and complementary functions of TRAF2 and TRAF3 in a ubiquitination cascade that activates NIK-dependent alternative NF-kappaB signaling. Nat. Immunol. 9, 1364–1370.
Yang, Z., 2008. I-TASSER server for protein 3D structure prediction. BMC Bioinformatics 40.
Zhang, Y., 2010. I-TASSER: fully automated protein structure prediction in CASP8. Proteins Struct. Funct. Bioinform. 77, 100–113.
Zhang, J.X., Ma, H.W., Sang, M., Hu, Y.S., Liang, Z.N., Ai, H.X., Zhang, J., Cui, X.W., Zhang, S.Q., 2010. Molecular structure, expression, cell and tissue distribution, immune evolution and cell proliferation of the gene encoding bovine (Bos taurus) TNFSF13 (APRIL). Dev. Comp. Immunol. 34, 1199–1208.
Zhang, J.X., Song, R., Sang, M., Sun, S.Q., Ma, L., Zhang, J., Zhang, S.Q., 2015. Molecular and functional characterization of BAFF from the Yangtze alligator (Alligator sinensis, Alligatoridae). Zoology 118, 325–333.
Zhang, J., Movahedi, A., Sang, M., Wei, Z., Xu, J., Wang, X., Wu, X., Wang, M., Yin, T., Zhuge, Q., 2017. Functional analyses of NDPK2 in Populus trichocarpa and overexpression of PtNDPK2 enhances growth and tolerance to abiotic stresses in transgenic poplar. Plant Physiol. Biochem. 117, 61.